JOURNAL OF AGRICULTURAL AND FOOD CHEMISTRY

ARTICLE

pubs.acs.org/JAFC

Preparation and Characterization of Novel Micro- and Nanocomposite Hydrogels Containing Cellulosic Fibrils

Fauze A. Aouada,*[,†] Márcia R. de Moura,[‡] William J. Orts,[§] and Luiz H. C. Mattoso[∥]

[†]Chemistry Institute, São Paulo State University, Araraquara Campus, Araraquara, SP 14800-900, Brazil

[‡]Physics Institute of São Carlos, University of São Paulo, São Carlos, SP 13560-970, Brazil

[§]Bioproduct Chemistry & Engineering Research Unit, USDA-ARS-WRRC, Albany, California 94710, United States

[∥]National Nanotechnology Laboratory for Agriculture, LNNA, Embrapa Agricultural Instrumentation, CNPDIA, São Carlos, SP 13560-905, Brazil

ABSTRACT: The main objective of this article was to report a simple, fast, and low cost strategy for the synthesis of micro- and nanocomposites by adding cellulose nanofibers, obtained by acid hydrolysis, and added to hydrogels as reinforcing agents. Specifically, when cellulose nanofibers were added to hydrogels, morphologic analyses showed significant decreases in pore size and formation of three-dimensional well-oriented porous microstructure. It was also observed that cellulose nanoparticles improved the mechanical and structural network properties without negatively impacting their thermal and hydrophilic properties. The value of maximum compressive stress was 2.1 kPa for the PAAm-MC, and it increased to 4.4 kPa when the cellulose nanofiber was incorporated into the hydrogel. By investigation of XRD patterns, it was found that the incorporation of cellulose nanofiber affected the crystallinity of PAAm-MC hydrogels, thus contributing to improvements in mechanical, structural, and hydrophilic properties of the PAAm-MC hydrogels.

KEYWORDS: cellulose nanofiber, PAAm-MC hydrogel, SEM, mechanical improvement, reinforcing effect, XRD characterization

INTRODUCTION

Cellulose microfibers, nanowhiskers, or nanofibers are rod-like nanocrystals with high-mechanical performance that have been successfully used as reinforcing fillers in a series of synthetic and natural polymeric matrices.[1−4] The use of cellulose as reinforcing material in composites or nanocomposites is a relatively new field in nanotechnology that has generated considerable interest in the past decade, especially in the biopolymer community.[5] The main reason for this reinforcement for cellulose nanofibers is due to its high aspect ratio of around 20−50, low density of 1.56 g/cm^3, high elastic modulus estimated at 145 GPa, and strength, reported to be 7500 MPa.[6]

Cellulose, considered an almost inexhaustible source of raw material, has been formed into fibers, films, gels, and micro- and nanoparticles for different applications.[7] It is the world's most abundant polysaccharide, applied in composites because it is natural, renewable, biodegradable, and highly biocompatible. Cellulose is biosynthesized by a diverse array of plants, trees, and even microbes and deposited into continuous elementary microfibrils formed by amorphous and crystalline parts, which can be about 5−10 nm in diameter. Microfibril length varies from 100 nm to several micrometers, depending on the source of cellulose.[8]

In recent years, an array of hydrogels with unique properties, including high mechanical and hydrophilic performance, has been developed for varied applications.[9−12] Hydrogels are insoluble polymeric materials containing a large number of hydrophilic groups capable of holding a large amount of water in their three-dimensional networks.[13] Hydrogels are composed of regions containing water and regions containing polymer chains; the water in a hydrogel network exists in a continuum state between two extremes.[14] Typically, at the micrometer range, hydrogels are best formed into particles and fibers because of their high specific surface that allows quick response to an external stimulus while minimizing steric hindrance.[15]

Methylcellulose is a simple cellulose derivative, with methyl groups substituted for hydrogens. This substitution disrupts the rigid crystalline structure, generally stabilized by strong intermolecular hydrogen bonding, and improves the polysaccharide's water affinity.[16] Acrylamide (AAm) and its derivatives are well-known for their hydrophilic and inert nature, which makes them suitable for medical and pharmaceutical applications.[17]

Recently, our research group has developed biodegradable polyacrylamide-methylcellulose (PAAm-MC) hydrogels for agricultural applications as a carrier vehicle for agrochemical controlled release.[12,18,19] In this study, the main objective was to report a simple, fast, and low cost strategy for the synthesis of micro- and nanocomposite hydrogels based on PAAm-MC and cellulose specimens with excellent mechanical and hydrophilic properties. Thermal stability was analyzed by thermogravimetric analysis, while morphological and structural properties were investigated by scanning electron microscopy and X-ray diffraction, respectively.

MATERIALS AND METHODS

Materials. The acrylamide (AAm) monomer was purchased from Fluka. *N*′,*N*-Methylene-bis-acrylamide (MBAAm), *N*,*N*,*N*′,*N*′-tetramethylethylenediamine (TEMED) and sodium persulfate (NaPS) were obtained from

Received: March 14, 2011
Accepted: July 27, 2011
Revised: July 27, 2011
Published: July 27, 2011

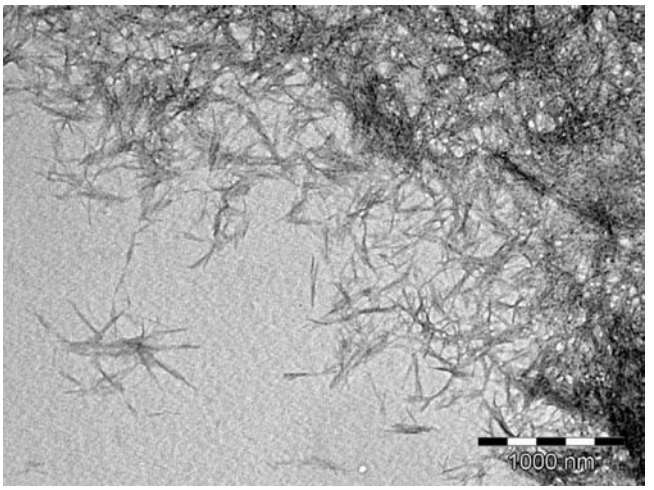

Figure 1. TEM image of cellulose nanofiber after the acid hydrolysis process.

Sigma. The polysaccharide MC was supplied by Aldrich. Commercial fibrous cellulose powder (trade name CF11) was purchased from Whatman International Ltd. (Maidstone, England). All reagents were used without any further purification. Double distilled water with resistance larger than 16 MΩ was used.

Miniaturization of Cellulose Fibers by Microfluidizer Processor before Acid Hydrolysis. To deagglomerate the commercial fibrous cellulose, CF11 was used in a Microfluidizer processor (model M-110EH-30 - Newton, MA, USA). The pressure utilized was 20,000 psi. The concentration of CF11 in the solution used was 5.0 wt %. This technique was utilized in order to facilitate the acid hydrolysis of the microfiber due to its better water dispersion.

Extraction of Cellulose Nanofibers (CNFibers) from Cellulose Microfibers (CMFibers). Extraction of CNFibers was carried out according to the modified methodology described by Favier et al.[20] and Orts et al.[21] Briefly, 10 wt % short cellulose fibers (after the Microfluidizer process) were stirred vigorously with 60 wt % sulfuric acid preheated at 45 °C for 75 min. Afterward, the mixture was quenched in cold water with continuous stirring. The resulting dispersion was centrifuged to 4400 rpm by 20 min, decanted, and washed with water continuously (at least 7 times) until the pH was above 1.5 and a stable dispersion formed. The resulting solution was water dialyzed in dialysis tubing (Spectrapor 2; MWCO 12,000−14,000; 45 mm flat width) for 4−5 days until the pH of the solution was between 5.5 and 6.5. CNFibers were recovered as a dispersion of approximately 0.55 g/100 mL water.

Preparation of Hydrogels. PAAm-MC hydrogels were obtained according to the procedure described by Aouada et al.[12,18,19] The hydrogels were obtained through polymerization/cross-linking of 6.0 wt % AAm and 8.55 μmol L^{-1} MBAAm in aqueous solution at room temperature containing 1.0 wt % MC in the presence of 0.10 mmol mL^{-1} NaPS initiator and 3.21 μmol mL^{-1} TEMED accelerator. After homogenization, the solution was purged by N_2 bubbling for 25 min. Finally, the resulting solution was quickly placed between two glass plates separated by a rubber gasket. After polymerization/cross-linking, the hydrogels were removed from the plates in membrane form and immersed in deionized water to remove the unreacted chemicals, e.g., monomers, catalyst, and initiator.

Incorporation of Cellulose Structures into PAAm-MC Hydrogels. Dry preweighed PAAm-MC hydrogel samples were immersed in cellulose micro- and nanofiber aqueous solution at pH ≈7.1 (0.55 wt %) for 72 h. The solutions were maintained at controlled temperature (25.0 ± 0.1 °C) using a thermostatic bath. The notations

Scheme 1. (a) Formation of Cross-Linked Network Structures Based on PAAm and MC Using MBAAm and TEMED as the Cross-Linker and Catalyst Agent, Respectively, and (b) Cellulose Micro and Nanofibers Anchored in PAAm-MC Hydrogels[a]

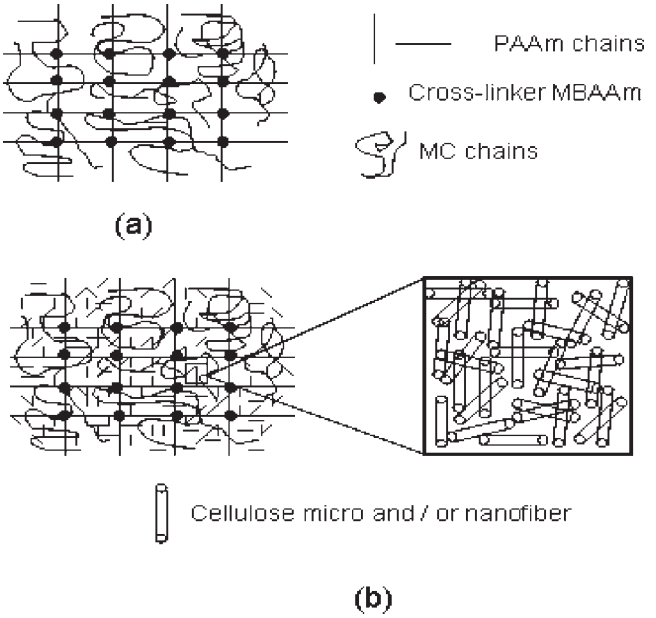

[a] [AAm] = 6.0 wt %; [MC] = 1.0 wt %; [MBAAm] = 8.55 μmol L^{-1}; [TEMED] = 3.21 μmol mL^{-1}; and [NaPS] = 0.10 $m$mol mL^{-1}.

PAAm-MC-MicFib and PAAm-MC-NanFib will be used to characterize the PAAm-MC hydrogels containing cellulose micro- and nanofiber, respectively.

Morphological Investigation by Scanning Electron Microscopy. Scanning electron microscopy (SEM) was used to investigate the morphological properties of PAAm-MC hydrogels with and without cellulose specimens. Hydrogels were frozen in liquid nitrogen and lyophilized for 24 h at −55 °C. This procedure was used to ensure that the swollen structure of the hydrogel did not change as a result of freezing. After the lyophilization process, the hydrogels were then deposited directly onto aluminum stubs using two-sided adhesive carbon tabs (Pelco, Redding, CA), and their surface was coated with gold−palladium in a Denton Desk II (Denton, NJ) sputter coating unit for approximately 60 s at 20 μA and 75 mTorr. The micrographs were obtained using a Hitachi S-4700 field emission SEM using 7.0 kV secondary electrons.

Swelling Degree (SD) Measurements. For the swelling measurements, approximately 0.01 g of hydrogel was immersed in 20 mL of deionized water and cellulose micro- and nanofibers, and kept static for 72 h. To measure the swelling degree, the hydrogel was carefully taken out from solution, wiped with a filter paper for the removal of free surface water, and then weighed. The degree of swelling was determined through the ratio between the weights of the swollen and dry hydrogel. Averaged values were calculated from four different measures; error bars indicate the standard deviation (n = 4).

Mechanical Properties. An Instron Model 5500R (Canton, MA), equipped with a 100 N load cell, was used for measuring the mechanical properties of the swollen hydrogels through uniaxial compression. Hydrogel compression was measured using a 1.27 cm diameter cylindrical probe. The probe was attached to the upper jaw of the Instron machine. The crosshead speed was 12.0 mm min^{-1}. The measurements were conducted up to 30% compression of the hydrogel. In this case, the maximum compressive stress (σ_{max}) of hydrogels was recorded.

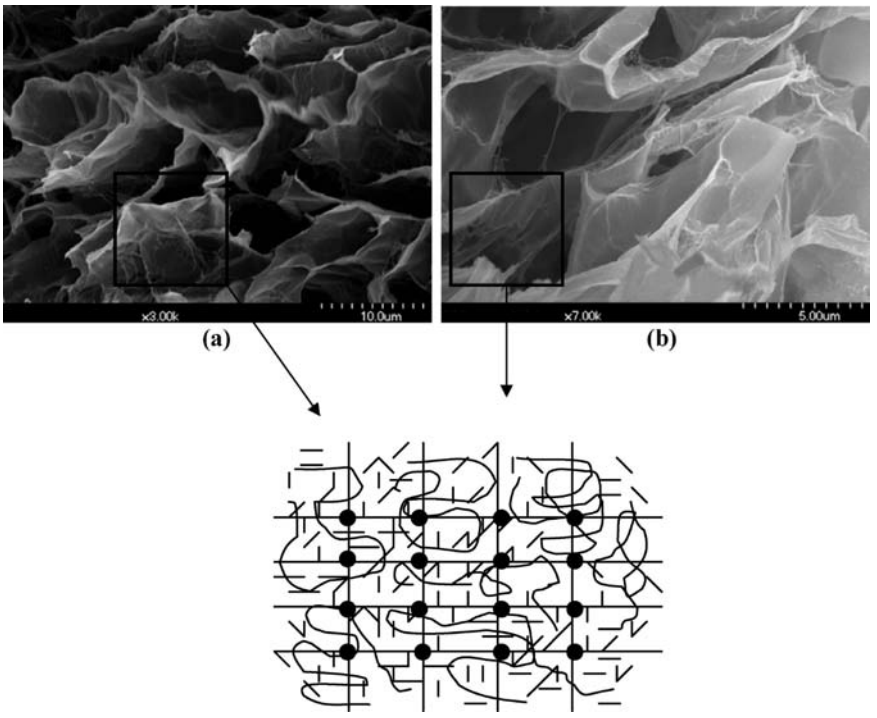

Figure 2. SEM micrographs of (a) PAAm-MC-MicFib and (b) PAAm-NanFib hydrogels. The morphological observations were used to assist in proposing Scheme 1.

The results shown are the mean values of six independent measurements, and the error bars indicate the standard deviation ($n = 6$).

The compressive stress (σ) and modulus of elasticity (E) properties were calculated by eq 1[22]

$$\sigma = \frac{F}{A} = E(\lambda - \lambda^{-2}) \quad (1)$$

where F is the force, and A is the cross-sectional area of the strained specimen (λ).

Thermogravimetric Analysis. A TGA-Q500 (TA Instruments, New Castle, DE, USA) thermogravimetric analyzer was used to characterize the thermal stability of the hydrogels. Each 5−8 mg hydrogels were performed in the temperature range 20−600 °C, heating rate of 10 °C/min, and nitrogen flow of 60 mL min^{-1}.

Structural Characterization by X-ray Diffraction. X-ray hydrogel diffraction analyses were performed with a Philips 1820 diffractometer [λ (Cu $K_{\alpha 1}$) = 0.15406 nm] operated at 45 kV and 40 mA at a scanning rate of 0.5°/min.

Transmission Electron Microscopy (TEM). Transmission Electron Microscopy (TEM) (Jeol 100 C, Tokyo, Japan) was applied to confirm the extraction of the cellulose nanofiber from cellulose microfiber through acid hydrolysis. Diluted cellulose nanofiber suspensions were sonicated for 2 min for better particle dispersion and to prevent agglomeration on the copper grid. One drop of the suspension was put on carbon-coated copper grid and then dried at room temperature for TEM analysis.

Fourier Transform Infrared (FTIR) Spectroscopy. Spectra of nanofibers, PAAm-MC and PAAm-MC-NanFiber hydrogels, in the range of 4000 cm^{-1} to 400 cm^{-1} were recorded on a Fourier transform infrared spectroscope (Perkin-Elmer, model Spectrum Paragon 1000). The samples were dried under vacuum until they reached a constant weight. Powdered samples were prepared into pellets with KBr (1 wt %). To reach a resolution of 2 cm^{-1}, 128 scans were acquired for each spectrum.

RESULTS AND DISCUSSION

Acid Hydrolysis of Microfibers to Obtain Cellulose Nanofibers. According to Qiu et al.,[23] the cellulose CF11 (from Whatman, Inc.) is an excellent source of pure cellulose microfibers with the following dimensions: 50−350 μm in length and 20 μm in diameter. After sulfuric acid hydrolysis, a highly stable suspension of hydrolyzed cellulose nanofibers was obtained from CF11. The opalescent suspension was the first indication of cellulose nanofiber extraction. The efficiency of the acid hydrolysis treatment was confirmed by the TEM technique (Figure 1) in which nanostructures with nanometer dimensions can be visualized. These morphologies have been previously reported by Zhang et al.[24] Additionally, the network-structured cellulose nanocrystals were observed to exhibit micrometer-scale dimensions along both their length and width. Similar cellulose nanocrystals with rod, sphere, and network morphologies were observed by Lu and Hsieh.[25] These authors attributed the network organization to the strong H-bonding among the cellulose nanocrystals, which overcomes the repulsion of surface negative charges, hence leading to the formation of self-assembled porous networks.

Hydrogel Formation and Morphological Observations. Hydrogels have been attracting a great deal of research attention due to their intriguing properties and applications, e.g., personal care products, agriculture, and biomedical uses.[26] Hydrogels are three-dimensional hydrophilic macromolecular networks that can absorb water many times their dry mass and significantly expand in volume without losing their chemical stability.

However, some hydrogels exhibit limitations, including limited mechanical properties and uncertain biodegradability. To overcome this problem, several efforts have been proposed such as the formation of semi-interpenetrating network (semi-IPN) hydrogels through the copolymerization between natural and

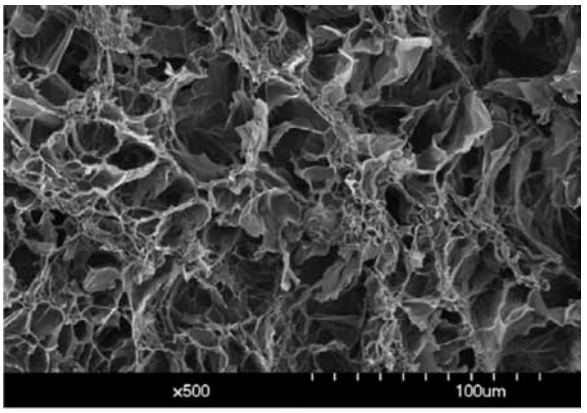

(a)

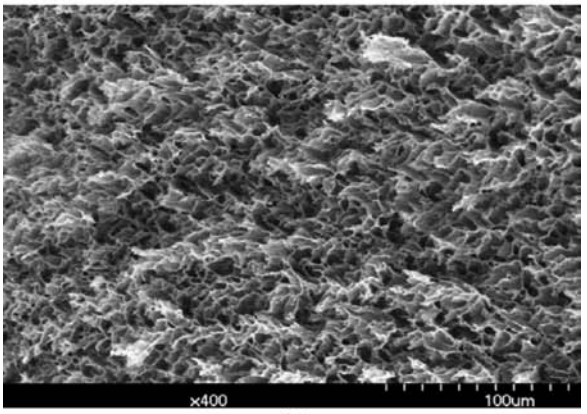

(b)

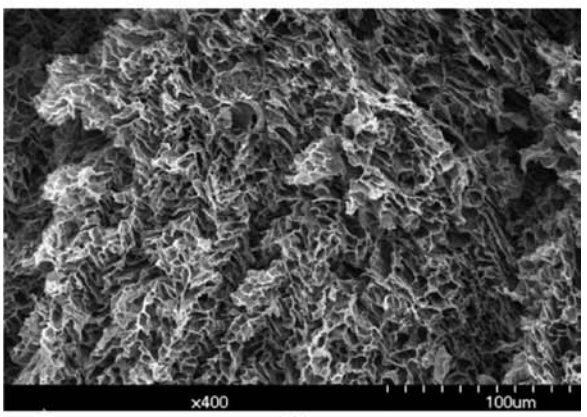

(c)

Figure 3. SEM micrographs of (a) PAAm-MC at 500× magnification, (b) PAAm-MC-MicFib, and (c) PAAm-NanFib hydrogels. Both b and c micrographs were obtained at 400× magnification.

synthetic monomers. For example, a hydrogel formed by copolymerization of acrylamide and methylcellulose has been shown to be a good alternative.[19] Another effective strategy is the inclusion of micro- and nanostructured cellulose in hydrogels, which can be added as reinforcement to improve the mechanical properties, biodegradability, and thermal stability without compromising their hydrophilic properties. Good reinforcement is attributed to the improved dispersion of the nanoscale fibers in the hydrogel matrix because of increased contact surface area between the hydrogel chains and fiber structures. This is promoted by increased hydrogen bonding of the cellulose fibers with the hydrogel matrixes. In this sense, Zhou and Wu[27] emphasized that few natural cellulose nanofibers with biocompatible and biodegradable properties have been tried in reinforcing nanocomposite hydrogels because highly swollen hydrogels are normally very brittle because of the lack of an efficient energy dissipation mechanism and irregular distribution of cross-linking points.

Scheme 1a presents the formation of cross-linked network structures based on PAAm and MC using *N*′,*N*-methylene-bisacrylamide (MBAAm) and *N*,*N*,*N*′,*N*′-tetramethylethylene-diamine (TEMED) as the cross-linker and catalyst agent, respectively. Possible conformational arrangements are shown in Scheme 1b, where the strong interactions between cellulose-MC segments and cellulose-PAAm chains are expected due to the structural and chemical similarities between these entities. Scheme 1 was initially proposed after the morphological observation of PAAm-MC nanocomposite hydrogels in Figure 2.

After their formation, nanocomposite hydrogels were kept in a water reservoir confirming that their chemical integrity was preserved for at least 6 months. In these nanocomposites, the cellulose nanofibers were effectively anchoring to the hydrogel network because no trace of cellulose in the water reservoir was detected by refraction index measurements.

Figure 3a depicts the SEM micrograph of a PAAm-MC hydrogel swollen in water, whereby a highly porous structure with well-defined shapes exhibiting some spread in pore size was observed. The presence of cellulose specimens causes a significant decrease in pore size, and the formation of three-dimensional well-oriented pore structure can be observed (Figure 3b and c). This trend is possibly related to the fact that the cellulose nanofibers are distributed around and inside the three-dimensional porous material. This effect is best demonstrated by an analysis of further enlarged SEM micrographs (Figure 4). Also, the cross-section images did not display any noticeable change from the top to the bottom of each sample, indicating that the structure of the samples was symmetric across the cross-section of the samples.[28]

Variation in morphologic properties may imply changes in the physical−chemical properties of the hydrogels. The influence of the addition of cellulose nanofibers on the hydrophilic properties of PAAm-MC hydrogels will now be discussed.

Hydrophilic Properties from SD Measurements. Figure 5 shows that the presence of cellulose nanofibers in the hydrogels provoked a considered variation in the hydrophilic properties (SD values) of the hydrogels. The highest water uptake was observed for PAAm-MC hydrogels, i.e., without confined cellulose specimens. Thus, it is possible to affirm that the PAAm-MC hydrogel is more hydrophilic than PAAm-MC-MicFib and PAAm-MC-NanFib hydrogels. It is well established that when the hydrogel network becomes increasingly compact, the penetration of water molecules into the hydrogel becomes increasingly difficult. As a consequence, the hydrophilicity and consequently the water-absorption capability of the hydrogels decrease significantly, reflecting the decrease of swelling degree values.[18] Therefore, this is a good indication that the cellulose nanoparticle is acting as a reinforcing agent.

The nanoscale dimensions of the confined cellulose nanofiber is an important parameter for the hydrogel microstructure, whereby the submicrometer "crowding" of the hydrogel by cellulose fibers causes a reduction in the swelling degree index (SD). For example, PAAm-MC (or pure hydrogel) exhibited an

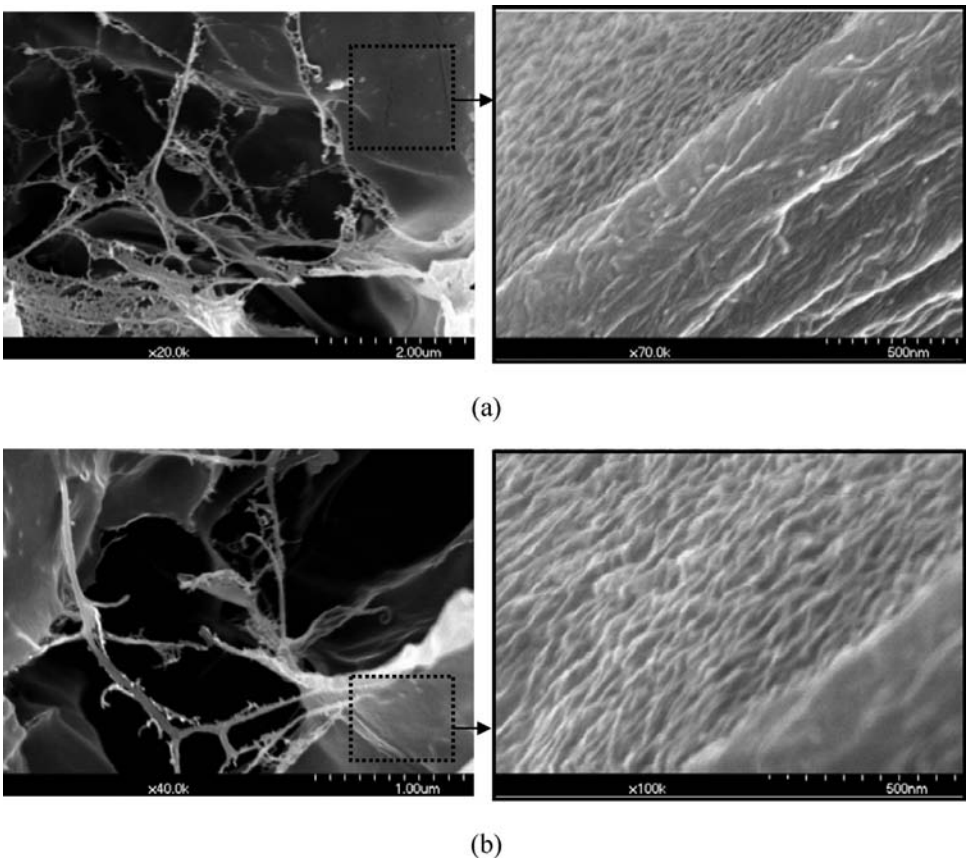

Figure 4. Enlarged SEM micrographs of (a) PAAm-MC-MicFib and (c) PAAm-NanFib hydrogels.

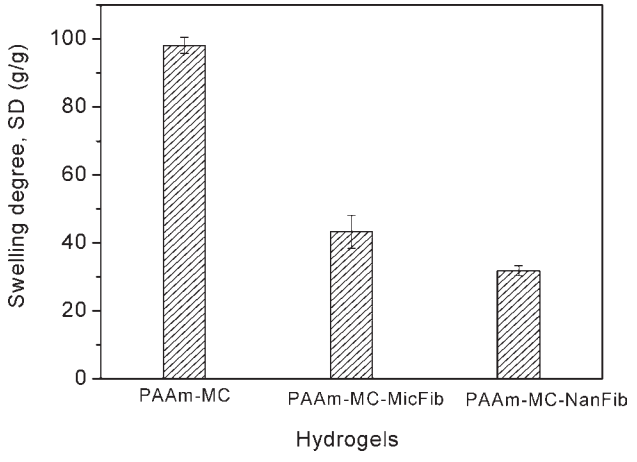

Figure 5. Dependence of swelling degree (SD) as a function of PAAm-MC hydrogel-type.

SD of 98 g/g; however, the SD values for PAAm-MC-MicFib and PAAm-MC-NanFib were 43.3 ± 4.9 and 31.8 ± 1.5 g/g, respectively.

Mechanical Reinforcement. The chemistry of cellulose is well-known and provides a rich variety of options for surface modification and materials engineering for many applications. The crystalline domains of the nanofibers possess very high strength, approximately in the order of or even greater than structural steel.[29] As a result, these nanocrystals are able to provide reinforcement to a variety of nanocomposites especially if there is some chemical interaction, such as hydrogen bonding, between the cellulose and the polymer matrix. Figure 6 shows the representative force−compressive stress deformation curves for the hydrogels tested with uniaxial compression, where good linearity between properties can be observed. The linear correlation indicates that elastic deformation occurred, i.e., the strain is recoverable after removing the applied stress.[30] Increases in both mechanical properties (maximum compressive stress (σ_{max}) and modulus of elasticity (E)) of the PAAm-MC hydrogels by the addition of cellulose specimens were found, as shown in Figure 7. The value of σ_{max} was 2.09 ± 0.07 kPa for the PAAm-MC, and it increased to 4.04 ± 0.12 kPa when the cellulose nanofiber was incorporated into the hydrogel. When the size of the cellulose nanoparticles was reduced from micro- to nanodimensions, the increase in σ_{max} was even more pronounced, i.e., 4.43 ± 0.06 kPa.

The variation of the modulus of elasticity of the different hydrogels demonstrated a similar behavior. This indicates that hydrogel formulations containing nanoscale cellulose fibers are more rigid than PAAm-MC or PAAm-MC-MicFib hydrogels. These results corroborate with the SD results and SEM observations, whereas the presence of cellulose nanostructures provoked the increase in rigidity of the hydrogel networks and the decrease in pore sizes.

Improvements in the mechanical properties of natural composites and polymers with the addition of low concentrations of cellulose microfibrils have been well documented. For example, Orts et al.[21] related that the addition of cellulose microfibrils to starch thermoplastic monofilaments has a significant effect on mechanical properties at low concentration. In agreement with

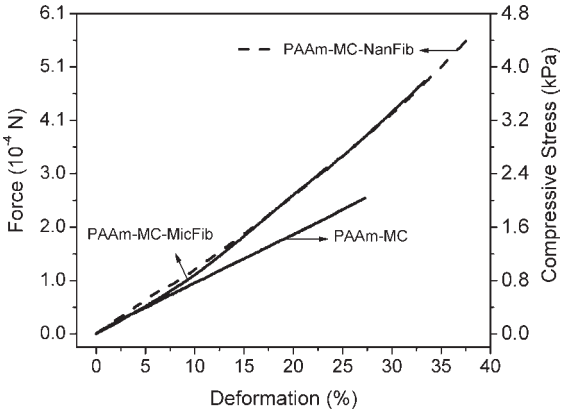

Figure 6. Dependence of (a) force and (b) compressive stress as a function of deformation for different PAAm-MC hydrogels.

Hubbe et al.,[29] cellulose nanocrystals possess significant molecular interaction with many polymer matrixes that allow them to improve the properties of the composites: cellulose crystals are rigid molecular rods and can impart significant strength and directional rigidity to a composite. Also, cellulose crystals have an embedded polymeric directionality that can be preferentially exploited for building new nanocomposites.

Characterization of Network Properties. In characterizing cross-linked hydrogels, the structural properties are typically characterized by the average molar mass between cross-links (M_C), the cross-link density (q), and the number of elastically effective chains totally included in a perfect network (V_e).[31] This is described in eqs 2 through 4, whereby

$$M_C = -V_1 d_P \frac{(V_S^{1/2} - V_{S/2})}{\ln(1 - V_S) + V_S + \chi V_S^2} \quad (2)$$

where V_1 is the molar volume of water (mL mol^{-1}), d_p is the polymer density (g mL^{-1}), V_s is the volume fraction of the polymer in the swollen gel, and χ is the Flory−Huggin's interaction parameter between solvent and polymer

$$q = \frac{M_0}{M_C} \quad (3)$$

where M_0 is the molar mass of the repeating unit.

$$V_e = \frac{d_P N_A}{M_C} \quad (4)$$

where N_A is the Avogadro's constant (or Avogadro's number).

Table 1 illustrates that both q and V_e values increased when M_c decreased, implying that when the cellulose particles are more confined, the reinforcement effect was favored. Concurrently, as discussed earlier, the swelling degree (SD) and the mechanical properties presented the same trend, hence confirming the confined nanostructure of the matrix. The hydrophilicity and polymer confinement of the swollen hydrogel is thus likely directly related to the M_c.[32] In this sense, the lowest value of M_c was found for the highest compact matrix, i.e., PAAm-MC-NanFib: $M_c = 7.2 \pm 0.6 \times 10^4$ g mol^{-1}; SD = 31.8 ± 1.5 g/g; $q = 0.98 \pm 0.09 \times 10^3$ g mol^{-1}; $V_e = 9.16 \pm 0.78 \times 10^{19}$ mol mL^{-1}.

Thermal Analysis. The TG and DTG curves of micro- and nanostructured PAAm-MC and PAAm-MC are shown in Figure 8. The PAAm-MC DTG thermogram showed mass loss at around 100−150 °C which is attributed to the water loss.

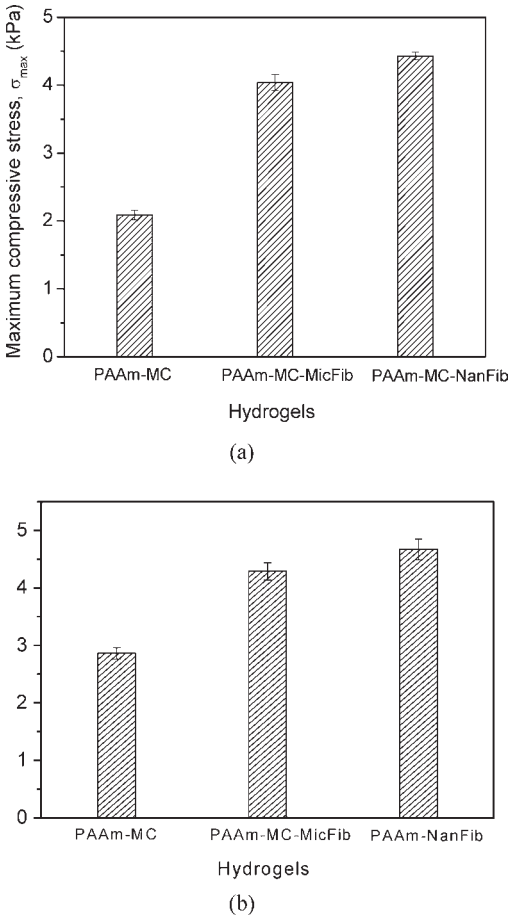

Figure 7. Dependence of (a) maximum compressive stress and (b) modulus of elasticity as a function of PAAm-MC hydrogel-type.

Additionally, according to Lu and Hsieh,[15] the thermally induced intra- and intermolecular imidization of the PAAm amide groups occurs above 200 °C, and the gradual mass loss at around 250 °C is consistent with the release of H_2O, NH_3, and CO_2 products from imidization; above 300 °C, the imides decomposed to form nitriles, and the polymeric main chain backbone formed hydrocarbons.

In the PAAm-MC thermograms, the temperature of the initial (T_{NF} beginning) and maximum degradation of the nitrile formations were observed at 290 and 355 °C, respectively. Additionally, there is another transition event in this region that corresponds to MC degradation. The TG and DTG thermograms for MC are shown in Figure 9, where it can be seen that the temperature of the maximum decomposition occurred at 280 °C.

The presence of cellulose nanoparticles confined into the PAAm-MC hydrogels did not significantly influence thermal degradation behavior, with only a slight decrease in T_{NF} beginning observed. The values of T_{NF} beginning for PAAm-MicFib and PAAm-NanFib were 289 and 286 °C (reduction of 1−4 °C in comparison to the T_{NF} for PAAm-MC).

XRD Characterization. Figure 10 shows the XRD patterns of the PAAm-MC hydrogels and PAAm-MC containing cellulose microfiber and cellulose nanofiber. It should be noted that PAAm-MC hydrogels presented broad featureless peaks in the range of around 10−30° due to their amorphous nature. However, XRD patterns of the cellulose micro- and cellulose

Table 1. Network Parameter of the Different PAAm-MC Hydrogels

hydrogels	SD (g/g)	M_c (10^4 g mol^{-1})	q (10^3 g mol^{-1})	V_e (10^{19} mol mL^{-1})
PAAm-MC	98.1 ± 2.4	48.8 ± 1.9	0.15 ± 0.01	1.36 ± 0.05
PAAm-MC-MicFib	43.3 ± 4.9	12.5 ± 2.4	0.57 ± 0.10	5.31 ± 1.07
PAAm-MC-NanFib	31.8 ± 1.5	7.2 ± 0.6	0.98 ± 0.09	9.16 ± 0.78

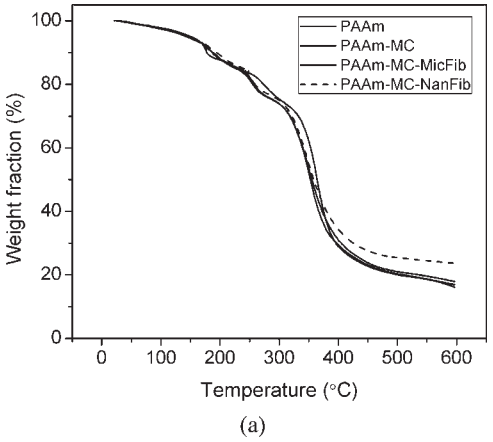

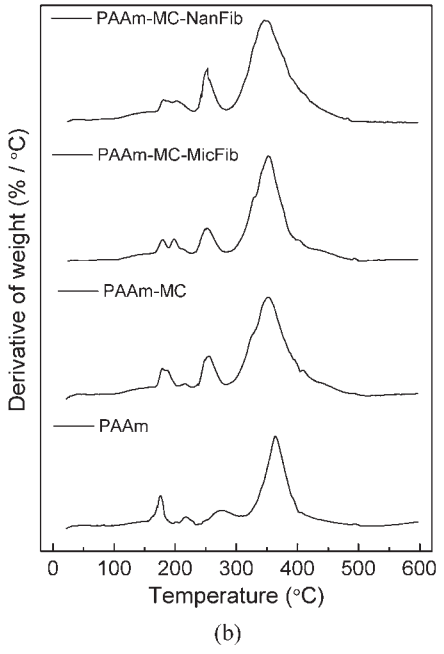

Figure 8. (a) TG and (b) DTG curves of the PAAm-MC, PAAm-MC-MicFib, and PAAm-MC-NanFib hydrogels.

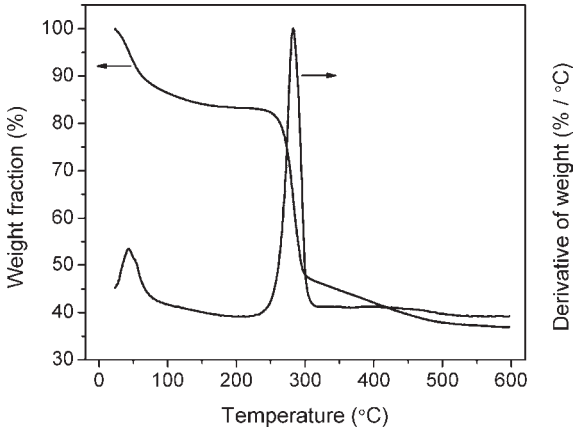

Figure 9. TG and DTG curves of the methylcellulose polysaccharide.

nanofibers exhibited some diffraction peaks. Specifically, diffraction peaks in the cellulose microfiber pattern (Figure 10a) are observed at 14.7°, 16.5°, 20.3°, 22.6°, and 34.1°, 2θ angle. The diffraction planes of cellulose, namely, 101, 101′, 021, 002, and 040, are present at 14.8°, 16.7°, 20.7°, 22.5°, and 34.6°, 2θ angle, respectively;[33] and the overlapping 11′0 and 110 peaks suggest that the structure of the cellulose corresponds to cellulose I.[34] The crystallinity index (CI) and crystallinity order index (COI) were calculated from diffraction peaks using proceeding described by Kaushik and Singh,[33] where the I_{002} and I_{Amorph} are the intensity diffractions at 22.5° and 14.7°, 2θ angle.[35] The CI and COI of cellulose microfibers were 68.2% and 65.5%, respectively. In addition, there are no significant changes in the PAAm-MC network structure detected by XRD analysis, and the PAAm-MC and PAAm-MC-MicFib patterns are very similar. Thus, the amorphous characteristics of the PAAm-MC are preserved after the confinement of the cellulose microfiber.

It was observed in Figure 10b that the amorphous diffraction peak at 14.7°, 2θ degrees in cellulose nanofibers disappeared; and due to the absence of this peak, it was not possible to determine the crystallinity index and crystallinity order index. However, this is indicative that the hydrolysis process was well done whereby processing increased the crystallinity of the cellulose. The increase in cellulose crystallinity after the chemical treatments has been reported by several authors. For instance, Chen et al.[36] observed a significant increase in crystallinity from 52.74% for the original wood fibers to 69.34% for the chemically purified cellulose fibers. The authors associated the increase to the removal of hemicellulose and lignin, which exist in amorphous regions, leading to the realignment of cellulose molecules. Kaushik et al.[37] related the increase in crystallinity to the removal of nanocellulosic polysaccharides and dissolution of amorphous zones, confirming that hydrolysis takes place preferentially in the amorphous region due to acidic dissolution, while the crystalline regions are more stable to chemical attack.

The incorporation of cellulose nanofibers affected the crystallinity of PAAm-MC hydrogels because relevant changes in their diffraction profiles were observed. The crystallinity increases also contributed to the improvement in mechanical, structural, and hydrophilic properties of the PAAm-MC hydrogels. The chemical treatment facilitated the formation of the 040 diffraction plane, whereas the diffraction peak in the cellulose nanofiber pattern 34.1°, 2θ angle is more accentuated in comparison to that of the cellulose microfiber shown in Figure 10a. Moreover, a novel diffraction peak was observed at 2θ = 31.8°, showing their interaction with the hydrogel matrix, possibly the formation of a novel diffraction plane with different conformational and

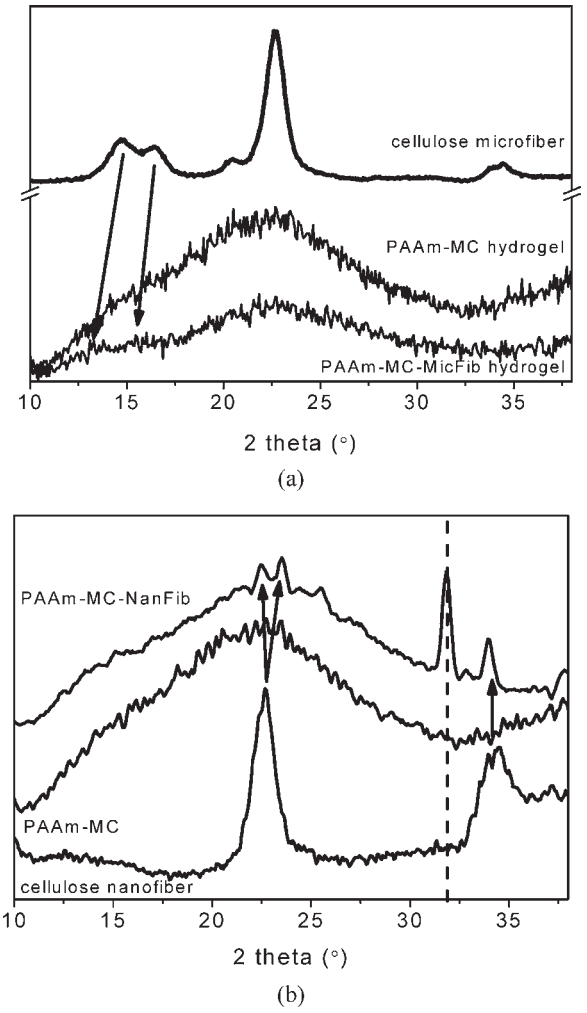

Figure 10. X-ray diffraction patterns of (a) cellulose microfiber, PAAm-MC, and PAAm-MC-MicFib; (b) cellulose nanofiber, PAAm-MC, and PAAm-MC-NanFib.

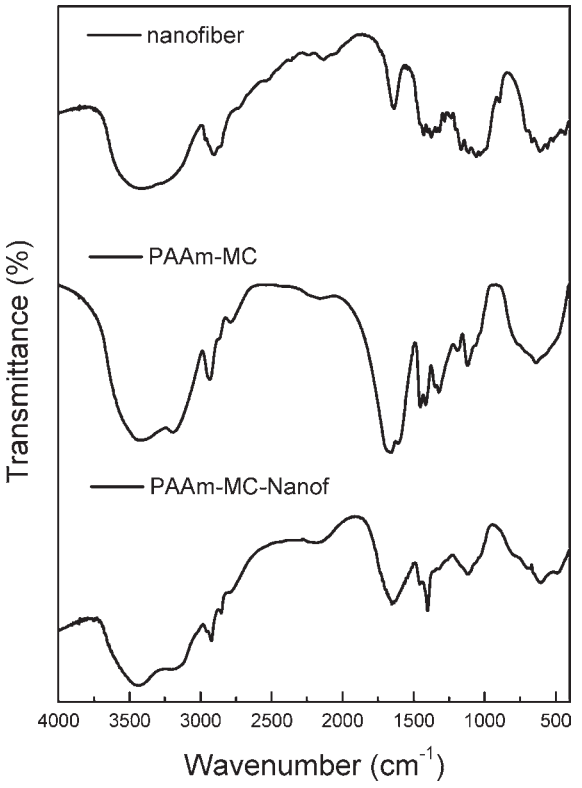

Figure 11. FTIR spectra of nanofiber, PAAm-MC, and PAAm-MC-NanFiber hydrogels.

energetic states. Finally, to our knowledge, we were the first to report this peak at $2\theta = 31.8°$.

Fourier Transform Infrared (FTIR) Spectroscopy. To assist the investigation of the new peak at $2\theta = 31.8°$ determined by XRD, the FTIR spectroscopy was used. FTIR spectra of nanofiber, PAAm-MC, and PAAm-MC-NanFiber hydrogels are presented in Figure 11. The PAAm-MC spectrum had bands at 3180 and 3442 cm^{-1} attributed to the combined peaks of the asymmetric and symmetric stretching vibrations of the primary amides −NH. Axial deformations relative to C−N bonds are observed at 1456 cm^{-1} and 1415 cm^{-1}. The intense band observed at 1668 cm^{-1} is related to the carbonyl stretching vibration (amide I). The peak at 1610 cm^{-1} is attributed to the N−H bending vibration (amide II) of the amide group and the adsorbed water molecular vibration (hydration water). It was observed in the PAAm-MC-NanFib spectrum that the absorption of carbonyl of the amide I of the nanocomposite shifted from 1668 cm^{-1} to 1646 cm^{-1}. According to Zhou and Wu,[27] the shift of the vibration of the carbonyl group to lower frequencies indicates inter- and/or intramolecular interactions between nanofibers and the polyacrylamide matrix through both hydrogen and covalent bonding. In addition, an intensification of the band at 1400 cm^{-1} can be observed in the PAAm-MC-NanFiber spectrum when compared to that of the PAAm-MC spectrum. Such intensification was attributed to planar deformation of H−C−H and O−C−H groups proceeding from the cellulose nanofibers. In this way, the main spectroscopic differences after nanofiber incorporation were observed in the range corresponding to the amide groups (present in PAAm and MBAAm), more specifically at the 3000−3500 cm^{-1} and 1220−1870 cm^{-1} regions.[38,39] This is indicative that the specific interaction that leads the formation of the XRD peak at $2\theta = 31.8°$ probably occurs between polar groups (from nanofibers) and amide groups.

In conclusion, in this article we successfully extracted the cellulose nanofibers from commercial fibrous cellulose powder (trade name CF11) processed by a Microfluidizer processor via acid hydrolysis. In summary, the presence of the cellulose micro- and nanofibers provoked pronounced changes in the hydrophilic, mechanical, structural, and morphological properties without diminishing their thermal stability. XRD patterns confirmed that the crystallinity of PAAm-MC-NanFib hydrogels increased in comparison to that of PAAm-MC. Using the SEM technique, it was observed that the presence of cellulose specimens causes a significant decrease in pore sizes and the formation of three-dimensional well-oriented pores. The results of the mechanical properties showed a significant increase in σ_{max} and E values when the cellulose microfiber was incorporated into the PAAm-MC hydrogel. These results supported the SD and SEM results, whereas the presence of cellulose structures provoked the increase in rigidity of the hydrogel networks and the decrease in pore sizes. Because of their biodegradability and biocompatibility, these novel nanocomposite hydrogels are promising

materials for different technological applications, such as carrier vehicles for controlled release (drugs, pesticides, and nutrients) and in biomedical engineering.

AUTHOR INFORMATION

Corresponding Author

*Tel: + 55 16 2107 2800. Fax: + 55 16 2107 2902. E-mail: (faouada@yahoo.com.br).

Funding Sources

We are grateful to CNPq, FAPESP, FINEP/LNNA, and Embrapa-Brazil for their financial support.

ABBREVIATIONS USED

A, cross-sectional area of the strained specimen (λ); AAm, acrylamide; CI, crystallinity index; CMFibers, cellulose microfiber; CNFibers, cellulose nanofibers; COI, crystallinity order index; d_p, polymer density; DTG, derivative thermogravimetric; E, modulus of elasticity; F, force; FTIR, Fourier transform infrared; M_C, average molar mass between cross-links; MC, methylcellulose; M_o, molar mass of the repeating unit; N_A, Avogadro's constant (or Avogadro's number); NaPS, sodium persulfate; PAAm, polyacrylamide; PAAm-MC-MicFib, polyacrylamide and methylcellulose hydrogels containing cellulose microfibers; PAAm-MC-NanFib, polyacrylamide and methylcellulose hydrogels containing cellulose nanofibers; q, cross-link density; SD, swelling degree; SEM, scanning electron microscopy; semi-IPN, semi-interpenetrating network; TEM, transmission electron microscopy; TEMED, N,N,N',N'-tetramethylethylene-diamine; TG, thermogravimetric; T_{NF}, temperature of the initial nitrile formation; V_1, molar volume of water; V_e, number of elastically effective chains totally included in a perfect network; V_s, volume fraction of the polymer in the swollen gel; XRD, X-ray diffraction; σ, compressive stress; σ_{max}, maximum compressive stress; χ, Flory−Huggin's interaction parameter between the solvent and polymer.

REFERENCES

(1) Buyanov, A. L.; Gofman, I. V.; Revelskaya, L. G.; Khripunov, A. K.; Tkachenko, A. A. Anisotropic swelling and mechanical behavior of composite bacterial cellulose−poly(acrylamide or acrylamide−sodium acrylate) hydrogels. *J. Mech. Behav. Biomed. Mater.* **2010**, *3*, 102–111.

(2) Wu, J.; Liang, S.; Dai, H.; Zhang, X.; Yu, X.; Cai, Y.; Zhang, L.; Wen, N.; Jiang, B.; Xu, J. Structure and properties of cellulose/chitin blended hydrogel membranes fabricated via a solution pre-gelation technique. *Carbohydr. Polym.* **2010**, *79*, 677–684.

(3) Chen, Y.; Liu, C.; Chang, P. R.; Cao, X.; Anderson, D. P. Bionanocomposites based on pea starch and cellulose nanowhiskers hydrolyzed from pea hull fibre: Effect of hydrolysis time. *Carbohydr. Polym.* **2009**, *76*, 607–615.

(4) Roohani, M.; Habibi, Y.; Belgacem, N. M.; Ebrahim, G.; Karimi, A. N.; Dufresne, A. Cellulose whiskers reinforced polyvinyl alcohol copolymers nanocomposites. *Eur. Polym. J.* **2008**, *44*, 2489–2498.

(5) Goetz, L.; Mathew, A.; Oksman, K.; Gatenholm, P.; Ragauskas, A. J. A novel nanocomposite film prepared from crosslinked cellulosic whiskers. *Carbohydr. Polym.* **2009**, *75*, 85–89.

(6) Paralikar, S. A.; Simonsen, J.; Lombardi, J. Poly(vinyl alcohol)/cellulose nanocrystal barrier membranes. *J. Membr. Sci.* **2008**, *320*, 248–258.

(7) Wang, Y.; Chen, L. Impacts of nanowhiskers on formation kinetics and properties of all-cellulose composite gels. *Carbohydr. Polym.* **2011**, *83*, 1937–1946.

(8) Zhou, C.; Wu, Q.; Yue, Y.; Zhang, Q. Application of rod-shaped cellulose nanocrystals in polyacrylamide hydrogels. *J. Colloid Interface Sci.* **2011**, *353*, 116–123.

(9) Xu, K.; Tan, Y.; Chen, Q.; An, H.; Li, W.; Dong, L.; Wang, P. A novel multi-responsive polyampholyte composite hydrogel with excellent mechanical strength and rapid shrinking rate. *J. Colloid Interface Sci.* **2010**, *345*, 360–368.

(10) Janovák, L.; Dékány, I. Optical properties and electric conductivity of gold nanoparticle-containing, hydrogel-based thin layer composite films obtained by photopolymerization. *Appl. Surf. Sci.* **2010**, *256*, 2809–2817.

(11) Moura, M. R.; de; Aouada, F. A.; Favaro, S. L.; Radovanovic, E.; Rubira, A. F.; Muniz, E. C. Release of BSA from porous matrices constituted of alginate-Ca^{2+} and PNIPAAm-interpenetrated networks. *Mater. Sci. Eng., C* **2009**, *29*, 2319–2325.

(12) Aouada, F. A.; Moura, M. R.; de; Orts, W. J.; Mattoso, L. H. C. Polyacrylamide and methylcellulose hydrogel as delivery vehicle for the controlled release of paraquat pesticide. *J. Mater. Sci.* **2010**, *45*, 4977–4985.

(13) Ahmed, E. M.; Aggor, F. S. Swelling kinetic study and characterization of crosslinked hydrogels containing silver nanoparticles. *J. Appl. Polym. Sci.* **2010**, *117*, 2168–2174.

(14) Milanchian, K.; Tajalli, H.; Gilani, A. G.; Zakerhamidi, M. S. Nonlinear optical properties of two oxazine dyes in aqueous solution and polyacrylamide hydrogel using single beam Z-scan. *Opt. Mater.* **2009**, *32*, 12–17.

(15) Lu, P.; Hsieh, Y. L. Organic compatible polyacrylamide hydrogel fibers. *Polymer* **2009**, *50*, 3670–3679.

(16) Stalling, S. S.; Akintoye, S. O.; Nicoll, S. B. Development of photocrosslinked methylcellulose hydrogels for soft tissue reconstruction. *Acta Biomater.* **2009**, *5*, 1911–1918.

(17) Dinu, M. V.; Perju, M. M.; Drăgan, E. S. Porous semi-interpenetrating hydrogel networks based on dextran and polyacrylamide with superfast responsiveness. *Macromol. Chem. Phys.* **2011**, *212*, 240–251.

(18) Aouada, F. A.; Chiou, B. S.; Orts, W. J.; Mattoso, L. H. C. Physicochemical and morphological properties of poly(acrylamide) and methylcellulose hydrogels: Effects of monomer, crosslinker and polysaccharide compositions. *Polym. Eng. Sci.* **2009**, *49*, 2467–2474.

(19) Aouada, F. A.; Pan., Z; Orts, W. J.; Mattoso, L. H. C. Removal of paraquat pesticide from aqueous solutions using a novel adsorbent material based on polyacrylamide and methylcellulose hydrogels. *J. Appl. Polym. Sci.* **2009**, *114*, 2139–2148.

(20) Favier, V.; Chanzy, H.; Cavaille, J. Y. Polymer nanocomposites reinforced by cellulose whiskers. *Macromolecules* **1995**, *28*, 6365–6367.

(21) Orts, W. J.; Shey, J.; Imam, S. H.; Glenn, G. M.; Guttman, M. E.; Revol, J. F. Application of cellulose microfibrils in polymer nanocomposites. *J. Polym. Environ.* **2005**, *13*, 301–306.

(22) Kadnaim, A.; Janvikul, W.; Wichai, U.; Rutnakornpituk, M. Synthesis and properties of carboxymethylchitosan hydrogels modified with poly(ester-urethane). *Carbohydr. Polym.* **2008**, *74*, 257–267.

(23) Qiu, W.; Zhang, F.; Endo, T.; Hirotsu, T. Effect of maleated polypropylene on the performance of polypropylene/cellulose composite. *Polym. Compos.* **2005**, *26*, 448–453.

(24) Zhang, G.; Elder, T. J.; Pu, Y. Q.; Ragauskas, A. J. Facile synthesis of spherical cellulose nanoparticles. *Carbohydr. Polym.* **2007**, *69*, 607–611.

(25) Lu, P.; Hsieh, Y. L. Preparation and properties of cellulose nanocrystals: Rods, spheres, and network. *Carbohydr. Polym.* **2010**, *82*, 329–336.

(26) Peng, G.; Xu, S.; Peng, Y.; Wang, J.; Zheng, L. A new amphoteric superabsorbent hydrogel based on sodium starch sulfate. *Bioresour. Technol.* **2008**, *99*, 444–447.

(27) Zhou, C.; Wu, Q. A novel polyacrylamide nanocomposite hydrogel reinforced with natural chitosan nanofibers. *Colloids Surf., B* **2011**, *84*, 155–162.

(28) Wu, Y. H.; Freeman, B. D. Structure, water sorption, and transport properties of crosslinked N-vinyl-2-pyrrolidone/N,N′-methylenebisacrylamide films. *J. Membr. Sci.* **2009**, *344*, 182–189.

(29) Hubbe, M. A.; Rojas, O. J.; Lucia, L. A.; Sain, M. Cellulosic nanocomposites: A review. *BioResources* **2008**, *3*, 929–980.

(30) Peppas, N. A.; Bures, P.; Leobandung, W.; Ichikawa, H. Hydrogels in pharmaceutical formulations. *Eur. J. Pharm. Biopharm.* **2000**, *50*, 27–46.

(31) Yildiz, U.; Kemik, O. F.; Hazer, B. The removal of heavy metal ions from aqueous solutions by novel pH-sensitive hydrogels. *J. Hazard. Mater.* **2010**, *183*, 521–532.

(32) Moura, M. R.; de; Aouada, F. A.; Guilherme, M. R.; Radovanovic, E.; Rubira, A. F.; Muniz, E. C. Thermo-sensitive IPN hydrogels composed of PNIPAAm gels supported on alginate-Ca^{2+} with LCST tailored close to human body temperature. *Polym. Test.* **2006**, *25*, 961–969.

(33) Kaushik, A.; Singh, M. Isolation and characterization of cellulose nanofibrils from wheat straw using steam explosion coupled with high shear homogenization. *Carbohydr. Res.* **2011**, *346*, 76–85.

(34) Bras, J.; Hassan, M. L.; Bruzesse, C.; Hassan, E. A.; El-Wakil, N. A.; Dufresne, A. Mechanical, barrier, and biodegradability properties of bagasse cellulose whiskers reinforced natural rubber nanocomposites. *Ind. Crop. Prod.* **2010**, *32*, 627–633.

(35) Klemm, D.; Heublein, B.; Fink, H. P.; Bohn, A. Cellulose: Fascinating biopolymer and sustainable raw material. *Angew. Chem., Int. Ed.* **2005**, *44*, 3358–3393.

(36) Chen, W.; Yu, H.; Liu, Y.; Chen, P.; Zhang, M.; Hai, Y. Individualization of cellulose nanofibers from wood using high-intensity ultrasonication combined with chemical pretreatments. *Carbohydr. Polym.* **2011**, *83*, 1804–1811.

(37) Kaushik, A.; Singh, M.; Verma, G. Green nanocomposites based on thermoplastic starch and steam exploded cellulose nanofibrils from wheat straw. *Carbohydr. Polym.* **2010**, *82*, 337–345.

(38) Tang, Q.; Wu, J.; Lin, J.; Li, Q.; Fan, S. Two-step synthesis of polyacrylamide/polyacrylate interpenetrating network hydrogels and its swelling/deswelling properties. *J. Mater. Sci.* **2008**, *43*, 5884–5890.

(39) Sivanantham, M.; Kesavamoorthy, R.; Sairam, T. N.; Sabharwal, K. N.; Raj, B. Stimulus response and molecular structural modification of polyacrylamide gel in nitric acid: A study by Raman, FTIR, and photoluminescence techniques. *J. Polym. Sci. Part B: Polym. Phys.* **2008**, *46*, 710–720.